



## TLN-4601 peripheral benzodiazepine receptor (PBR/TSPO) binding properties do not mediate apoptosis but confer tumor-specific accumulation

T. Bertomeu<sup>a</sup>, V. Zvereff<sup>a</sup>, A. Ibrahim<sup>a</sup>, S.P. Zehntner<sup>b</sup>, A. Aliaga<sup>c</sup>, P. Rosa-Neto<sup>c</sup>, B.J. Bedell<sup>b,c</sup>, P. Falardeau<sup>a</sup>, H. Gourdeau<sup>a,\*</sup>

<sup>a</sup>Thallion Pharmaceuticals Inc., 7150 Alexander-Fleming, Montréal, QC, H4S 2C8, Canada

<sup>b</sup>Biospective Inc., 6100 Royalmount, Montréal, QC, H4P 2R2, Canada

<sup>c</sup>McConnell Brain Imaging Centre, Montreal Neurological Institute, McGill University, 3801 University Street, Montréal, QC, H3A 2B4, Canada

### ARTICLE INFO

#### Article history:

Received 30 April 2010

Accepted 12 July 2010

#### Keywords:

Peripheral benzodiazepine receptor

Translocator protein

TLN-4601

Apoptosis

Tumor accumulation

### ABSTRACT

TLN-4601 is a farnesylated dibenzodiazepinone isolated from *Micromonospora* sp. with an anti-proliferative effect on several human cancer cell lines. Although the mechanism of action of TLN-4601 is unknown, our earlier work indicated that TLN-4601 binds the PBR (peripheral benzodiazepine receptor; more recently known as the translocator protein or TSPO), an 18 kDa protein associated with the mitochondrial permeability transition (mPT) pore. While the exact function of the PBR remains a matter of debate, it has been implicated in heme and steroid synthesis, cellular growth and differentiation, oxygen consumption and apoptosis. Using the Jurkat immortalized T-lymphocyte cell line, documented to have negligible PBR expression, and Jurkat cells stably transfected with a human PBR cDNA, the present study demonstrates that TLN-4601 induces apoptosis independently of PBR expression. As PBRs are overexpressed in brain tumors compared to normal brain, we examined if TLN-4601 would preferentially accumulate in tumors using an intra-cerebral tumor model. Our results demonstrate the ability of TLN-4601 to effectively bind the PBR *in vivo* as determined by competitive binding assay and receptor occupancy. Analysis of TLN-4601 tissue and plasma indicated that TLN-4601 preferentially accumulates in the tumor. Indeed, drug levels were 200-fold higher in the tumor compared to the normal brain. TLN-4601 accumulation in the tumor (176 µg/g) was also significant compared to liver (24.8 µg/g; 7-fold) and plasma (16.2 µg/mL; 11-fold). Taken together our data indicate that while PBR binding does not mediate cell growth inhibition and apoptosis, PBR binding may allow for the specific accumulation of TLN-4601 in PBR positive tumors.

© 2010 Elsevier Inc. All rights reserved.

### 1. Introduction

The peripheral benzodiazepine receptor (PBR; more recently known as the translocator protein or TSPO [1]) was originally discovered as an alternate binding site for the benzodiazepine diazepam (Valium<sup>®</sup>) [2]. It is found associated with components of the mitochondrial permeability transition (mPT) pore, which is a multiprotein complex located at the contact site between inner and outer mitochondrial membranes (OMM) (reviewed in [1,3]). The mPT pore is composed of the voltage-dependent anion channel (VDAC), the nucleotide adenine translocator (ANT) and the CsA-responsive Cyclophilin D (Cyp-D). However, there is still some controversy whether the PBR can be considered a component of the mPT pore [4]. Most of the PBR is located within the OMM where it regulates cholesterol transport and synthesis of steroid

hormones [5]. Overexpression of PBRs is documented in many tumor types including breast, colorectal, and prostate cancers [6–8] and their expression correlates with the degree of malignancy [9–12]. In addition, this overexpression is well established in gliomas where PBR density is elevated compared to normal cortex [13] and PBR ligands have been used clinically as imaging tools in the diagnosis of brain tumors [14,15].

TLN-4601 is a secondary metabolite produced by *Micromonospora* sp. This drug was discovered through Thallion's DECIPHER<sup>®</sup> platform, a genome scanning technique that allows the prediction of secondary metabolite production and structure, as well as facilitating their isolation [16,17]. Our early data indicated that TLN-4601 specifically binds the PBR [18]. Many PBR ligands have been reported to induce apoptosis [19–23], although the responsible molecular mechanism(s) are not clearly understood. One possible mechanism for this apoptosis induction could be mPT pore opening [24]. As TLN-4601 was shown to have a broad cytotoxic activity (low µM) when tested in the NCI 60 tumor cell line panel and has demonstrated *in vivo* antitumor activity in

\* Corresponding author. Tel.: +1 514 940 3600.

E-mail address: [hgourdeau@gmail.com](mailto:hgourdeau@gmail.com) (H. Gourdeau).

several xenograft models [18], we investigated whether it could induce apoptosis and whether TLN-4601 binding to the PBR is involved. We used both the Jurkat cell line (Jurkat WT), a cell line naturally devoid of PBR expression [25], and a stably human PBR transfected Jurkat cell line (Jurkat-PBR). Also, since PBRs are overexpressed in brain tumors compared to normal brain, we examined if TLN-4601 would preferentially target and accumulate in brain tumors using an intra-cerebral tumor model.

We show that both Jurkat WT and Jurkat-PBR are equally sensitive to TLN-4601 and that both undergo apoptosis to the same extent. Moreover, TLN-4615, a closely related analog that does not bind the PBR, also induces apoptosis. These data suggest that TLN-4601 mediated apoptosis does not involve its PBR-binding capacity. Using *in vivo* PET (positron emission tomography) imaging, we found that TLN-4601 could displace the PBR-specific ligand PK11195 from binding within the tumor. Moreover, a 200-fold and 11-fold greater accumulation of the drug was found within the tumor as compared both to normal brain tissue and plasma levels. We propose that the PBR-binding property of TLN-4601 favors drug accumulation within tumor cells overexpressing PBR, a promising property for an anticancer drug candidate.

## 2. Materials and methods

### 2.1. Cell culture

The human T-lymphocyte clone E6-1 cell line (Jurkat WT) was obtained from the American Type Culture Collection (ATCC; Manassas, VA). Jurkat WT were grown in suspension in RPMI-1640 supplemented with 10% heat-inactivated fetal bovine serum (FBS; WISENT Inc., QC, Canada) and maintained in a humidified atmosphere at 37 °C with 5% CO<sub>2</sub>. Jurkat cells stably expressing human PBR were a generous gift of P. Casellas (Sanofi-Aventis, Montpellier, France) and are described elsewhere [26]. They were grown in the same media supplemented with 500 µg/mL of G418 (Geneticin<sup>®</sup>; Gibco-BRL Life Technologies Inc.).

### 2.2. PBR ligand binding assay

Enriched mitochondrial membranes were prepared by mincing and homogenizing rat hearts in 20 volumes of ice-cold 50 mM Tris-HCl pH 7.5 using a PT 10-35 Polytron. After two 10 min centrifugations (1500 × *g* at 4 °C), the supernatant was further centrifuged for 20 min at 20,000 × *g*. The pellet was resuspended in 20 volumes of 50 mM Tris-HCl pH 7.5 and centrifuged at 48,000 × *g* for 20 min. Protein content in the pellet was measured with a Bradford protein assay (Bio-Rad Laboratories) with titration against BSA and aliquots stored at –80 °C.

Crude mitochondrial membranes (25 µg per well) were distributed onto Millipore HTS Multiscreen GF/B 96-well plates [27] pre-wet with 0.3% polyethyleneimine and washed with PBR-binding buffer (50 mM Tris-HCl pH 7.5 and 10 mM MgCl<sub>2</sub>). Binding assays were conducted in a final volume 300 µL PBR-binding buffer containing 1.6 nM [<sup>3</sup>H]PK11195 (84.8 Ci/mmol, Perkin Elmer) and increasing concentrations of TLN-4601 or TLN-4615 solubilised in 3 µL of DMSO. After 1 hr incubation at RT, filter plates were vacuum washed with PBR-binding buffer, dried and filters punched out into scintillation vials and bound radioactivity measured on a TriCARB 2800 liquid scintillation counter (Perkin Elmer, USA).

### 2.3. PBR expression

PBR expression in Jurkat WT and Jurkat-PBR was evaluated in a radioligand binding assay. Briefly, cells were washed in ice-cold PBS, resuspended in 300 µL of phosphate buffered saline (PBS) containing increasing amounts of [<sup>3</sup>H]PK11195 with or without

cold PK11195 to correct for specific binding. Nonspecific binding was determined in the presence of 100 µM concentration of unlabeled PK11195. Samples were incubated in triplicates for 2.5 h at 4 °C in GF/B Millipore HTS plates, washed once with PBS and filters counted as described above.

### 2.4. Cytotoxicity measurements

Exponentially growing Jurkat WT and Jurkat-PBR cells were seeded in 96-well plates (5000 cells in 150 µL). TLN-4601 and TLN-4615 were added in a volume of 50 µL to obtain final concentrations of 0, 0.1, 1, 3, 10 and 30 µM in RPMI-10% FBS and 0.05% DMSO. Following a 3-day incubation, XTT reagent was added and O.D. measurement were taken at 450 nm and 690 nm. Values represent corrected O.D. values (O.D. reading at 450 nm minus O.D. reading at 690 nm).

### 2.5. Cell lysis and Western blots

For dose-dependent studies, exponentially growing Jurkat WT and Jurkat-PBR cells were treated with 0 (DMSO only), 1, 3 and 10 µM TLN-4601 or TLN-4615 for 18 h. After treatment, cells were washed once with PBS, centrifuged and the cell pellet lysed in RIPA buffer (50 mM Tris-HCl pH 7.4, 1% Triton X-100, 1% sodium deoxycholate, 0.1% SDS, 150 mM NaCl and 1 mM EDTA) supplemented with phosphatase (cocktail Set II, Calbiochem) and protease (Complete Mini, Roche) inhibitors. Proteins (20 µg) were separated by 12% SDS-PAGE, transferred onto nitrocellulose membranes, blocked in 5% nonfat dry milk in 0.1% TBS-tween 20 and probed with cleaved caspase 3 antibody (CS-9661, Cell Signaling Technology, Beverly MA) followed by PARP antibody (CS-9542, Cell Signaling Technology). Primary antibodies were detected with horseradish peroxidase-conjugated secondary antibodies (Jackson ImmunoResearch Laboratories) and chemiluminescence HRP substrate (Millipore, Mississauga, ON, Canada).

A time dependent response was evaluated after exposing Jurkat WT and Jurkat-PBR cells to 10 µM TLN-4601 for up to 6 h. Cytosolic and mitochondrial fractionation was performed by selective digitonin permeabilization [28]. Briefly, 2 × 10<sup>6</sup> cells were resuspended in 200 µL of ice-cold permeabilization buffer (200 µg/mL digitonin, 80 mM KCl and 1 mM EDTA in 1× PBS) and incubated on ice for 5 min. The lysate was centrifuged at 800 × *g* for 5 min and the supernatant was recovered as the cytosolic fraction. The pellet was then extracted with 200 µL 50 mM Tris-HCl pH 7.5, 150 mM NaCl, 2 mM EGTA, 2 mM EDTA, 0.2% Triton X-100, 0.3% NP-40 and protease inhibitors for 10 min while rocking slowly. After centrifugation at 13,000 × *g* for 5 min, the supernatant was recovered as the mitochondrial fraction.

Cytosolic and mitochondrial proteins (20 µg) were separated by 12% SDS-PAGE, transferred onto nitrocellulose membranes, blocked in 5% nonfat dry milk in 0.1% TBS-tween 20 and probed with Cytochrome C (BD-556433, Becton, Dickinson and Company), VDAC (SC-58649, SantaCruz Biotechnology) and GAPDH (SC-32233, SantaCruz Biotechnology, Santa Monica, CA) specific antibodies. Primary antibodies were detected with horseradish peroxidase-conjugated secondary antibodies (Jackson ImmunoResearch Laboratories) and chemiluminescence HRP substrate (Millipore, Mississauga, ON, Canada).

### 2.6. Mitochondrial membrane potential

Jurkat WT and Jurkat-PBR cells were incubated into 5 mL BD FACS tubes (800,000 cells in 2 mL of RPMI + 10% FBS) and kept in a CO<sub>2</sub> incubator. At the appropriate time, so that all incubation times of our time-course ended together, TLN-4601 at a final concentration of 10 µM was added and cells gently mixed. Fifteen min before

final incubation time, 1  $\mu\text{L}$  of 50  $\mu\text{M}$  TMRE (T-669; Invitrogen Corporation) was added and tubes vortexed. Tubes were transferred on ice protected from light and immediately analyzed by FACS. Values shown represent the median fluorescence normalized for untreated cells. The experiment was done in triplicates.

### 2.7. DNA fragmentation analysis

Exponentially growing Jurkat WT and Jurkat-PBR cells were exposed to 10  $\mu\text{M}$  TLN-4601 for up to 24 h. At different incubation times, cells were harvested, their viability measured by trypan blue exclusion, they were centrifuged, and the cell pellet was resuspended in 400  $\mu\text{L}$  of lysis buffer (5 mM Tris-HCl pH 7.5, 5 mM EDTA and 0.5% Triton X-100). Detergent soluble DNA was extracted as previously described [29]. Samples were loaded on a TBE 1  $\times$  1.5% agarose gel and small MW DNA fragments were visualized by ethidium bromide staining.

### 2.8. Preparation and surgical implantation of spheroids

Rat C6 glioma cells were purchased from the ATCC (Manassas, VA) and grown in DMEM supplemented with 10% FBS, 125 U/mL penicillin G, 125  $\mu\text{g}/\text{mL}$  streptomycin sulfate, and 2.2  $\mu\text{g}/\text{mL}$  amphotericin B. Upon reaching confluency, spheroids were prepared using the hanging drop method previously described by Del Duca et al. [30]. Briefly, 20  $\mu\text{L}$  drops of DMEM containing 15,000 rat C6 glioma cells (obtained from exponentially growing cultures) were suspended from the lids of culture dishes and the resulting aggregates formed after 72 h were transferred to culture dishes base-coated with agar. The resulting spheroids were adequate for *in vivo* implantation after 48 h of incubation on agar.

Male, Sprague-Dawley rats (250–300 g) were anesthetized with 50 mg/kg ketamine and 10 mg/kg xylazine. The right cortical surface in the parietal-occipital region was exposed by craniectomy using a high-powered drill and the underlying dura and its vessels were carefully removed under a surgical microscope. A piece of the cortex was removed to expose the underlying white matter and a single spheroid was placed into the surgical defect. The craniectomy was covered with bone wax and the overlying skin sutured. A total of 6 animals were used for these studies. Animal studies were conducted in accordance with the guidelines provided by the Canadian Council for Animal Care and with the prior approval from McGill University Animal Care Committee.

### 2.9. *In vivo* [ $^{11}\text{C}$ ]PK11195 PET imaging in rats

*In vivo* PET studies were performed 14 days post-tumor implantation. PET imaging studies were performed while the animal was anesthetized with 2% isoflurane administered via nose cone and placed in the supine position on the bed and at the center of the field-of-view of the Siemens/CTI Concorde R4 microPET scanner (Siemens/CTI Concorde, Knoxville, TN, USA). Each dynamic PET study lasted 60 min and was initiated with an IV bolus administration of [ $^{11}\text{C}$ ](R)-PK11195 (7.1–12.7 MBq) radioligand, a specific and high-affinity PBR ligand. Receptor occupancy studies were performed by acquisition of [ $^{11}\text{C}$ ](R)-PK11195 images prior to and 60 min following bolus IV infusion (30 mg/kg) followed by continuous IV infusion (5 mg/h/kg), which lasted throughout the scan. Attenuation correction factors, for each rat, were determined using a 10 min  $^{57}\text{Co}$  transmission scan acquired immediately prior to the dynamic scan. In addition, all images were scatter corrected.

### 2.10. PET data analysis

Images were reconstructed using filtered back-projection, and time-activity curves (TACs) were obtained from regions-of-interest

(ROIs) in the tumor (target region), brain (reference region), and cerebellum (reference region). Binding potential (B.P.) was obtained by modeling the TACs using the simplified reference tissue method [31]. The PET outcome measure B.P. expresses the ratio between the total number of PBRs ( $B_{\text{max}}$ ) and PK11195 dissociation constant ( $K_d$ ) in the steady-state condition. Paired *t*-test comparing binding potentials obtained before and after treatment were computed using the R statistics software ([www.r-project.org](http://www.r-project.org)). *P*-values less than or equal to 0.05 were considered statistically significant.

### 2.11. Plasma and tissue drug levels

Following the completion of the *in vivo* studies, animals were sacrificed by anaesthetic overdose and decapitated. Blood samples were collected by cardiac puncture into tubes containing  $\text{K}_2\text{-EDTA}$  as an anticoagulant. Samples were centrifuged 10,000  $\times$  g for 10 min and plasma samples were collected and stored at  $-80^\circ\text{C}$  until analysis. Brain, liver, and tumors were snap-frozen in liquid  $\text{N}_2$  and stored at  $-80^\circ\text{C}$  until analysis. TLN-4601 was extracted with acetone and quantified by HPLC-MS/MS as previously described [18].

## 3. Results

### 3.1. TLN-4601 is a PBR binder while the analog TLN-4615 is not

TLN-4601 (Fig. 1A, upper structure) is a farnesylated dibenzodiazepinone with a structure reminiscent of cholesterol and diazepam, two known PBR ligands. TLN-4615 (Fig. 1A, lower structure), a closely related analog of TLN-4601 differs by having

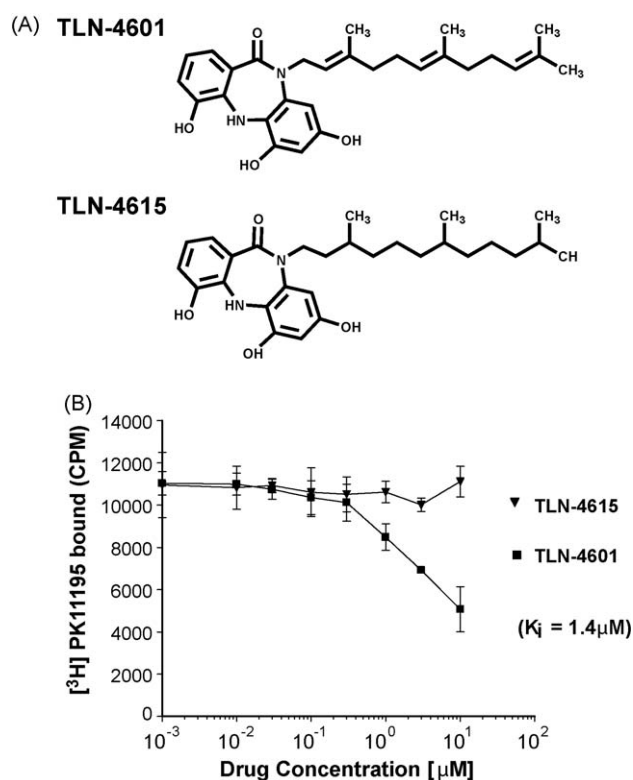


**Fig. 1.** The farnesyl side-chain of TLN-4601 partly mediates PBR-binding. (A) Molecular structure of TLN-4601 and TLN-4615, a semi-synthetic derivative. (B) Radioligand binding assay of TLN-4601 and TLN-4615 displacing or not [ $^3\text{H}$ ]PK11195 from PBR enriched from Wistar rat hearts. TLN-4601 and TLN-4615 were tested at 0.01, 0.03, 0.1, 0.3, 1, 3 and 10  $\mu\text{M}$  and the concentration of [ $^3\text{H}$ ]PK11195 was 1.6 nM. Assays were done in triplicates and error bars represent standard deviation (S.D.).

the farnesyl side chain saturated. As previously shown [18], TLN-4601 is a PBR ligand ( $K_i = 1.4 \mu\text{M}$ ), measured by displacement of tritiated PK11195 from rat heart enriched mitochondrial membranes (Fig. 1B). Interestingly, TLN-4615 does not bind the PBR (Fig. 1B) indicating that the side chain, and not the benzodiazepine ring as originally hypothesized, mediates PBR binding.

### 3.2. TLN-4601 inhibits cell growth and induces apoptosis independently of PBR expression

Saturation binding studies using the specific and selective PBR ligand [ $^3\text{H}$ ]PK11195 indicated that while Jurkat WT cells are devoid of functional PBR expression, Jurkat-PBR cells express elevated levels of functional receptor (Fig. 2A). The effect of TLN-4601 and the non-PBR binding analog, TLN-4615 on the cell growth of Jurkat WT and Jurkat-PBR was then assessed. Increasing concentrations

of TLN-4601 resulted in a dose-dependent decrease in cell growth as measured by a reduction in the formation of the soluble formazan dye (Fig. 2B, left panel). Both cell lines were equally sensitive to TLN-4601, calculated  $\text{IC}_{50}$  around  $10 \mu\text{M}$ , suggesting that PBR expression does not correlate with the antiproliferative activity of TLN-4601. Moreover, TLN-4615, which does not bind the PBR was as effective as TLN-4601 to inhibit cell growth, calculated  $\text{IC}_{50}$  around  $5 \mu\text{M}$  (Fig. 2B, right panel).

Some PBR ligands have been shown to induce apoptosis. We were thus interested to see if TLN-4601 could induce apoptosis and document if the inhibition of cell growth in the absence of PBR expression was mediated through a similar mechanism as in cells expressing PBR. As shown in Fig. 2C (left panel), TLN-4601 exposure resulted in caspase 3 activation and PARP cleavage to a similar extent in both Jurkat WT and Jurkat-PBR. Interestingly, TLN-4615 which does not bind the PBR and inhibits cell growth of

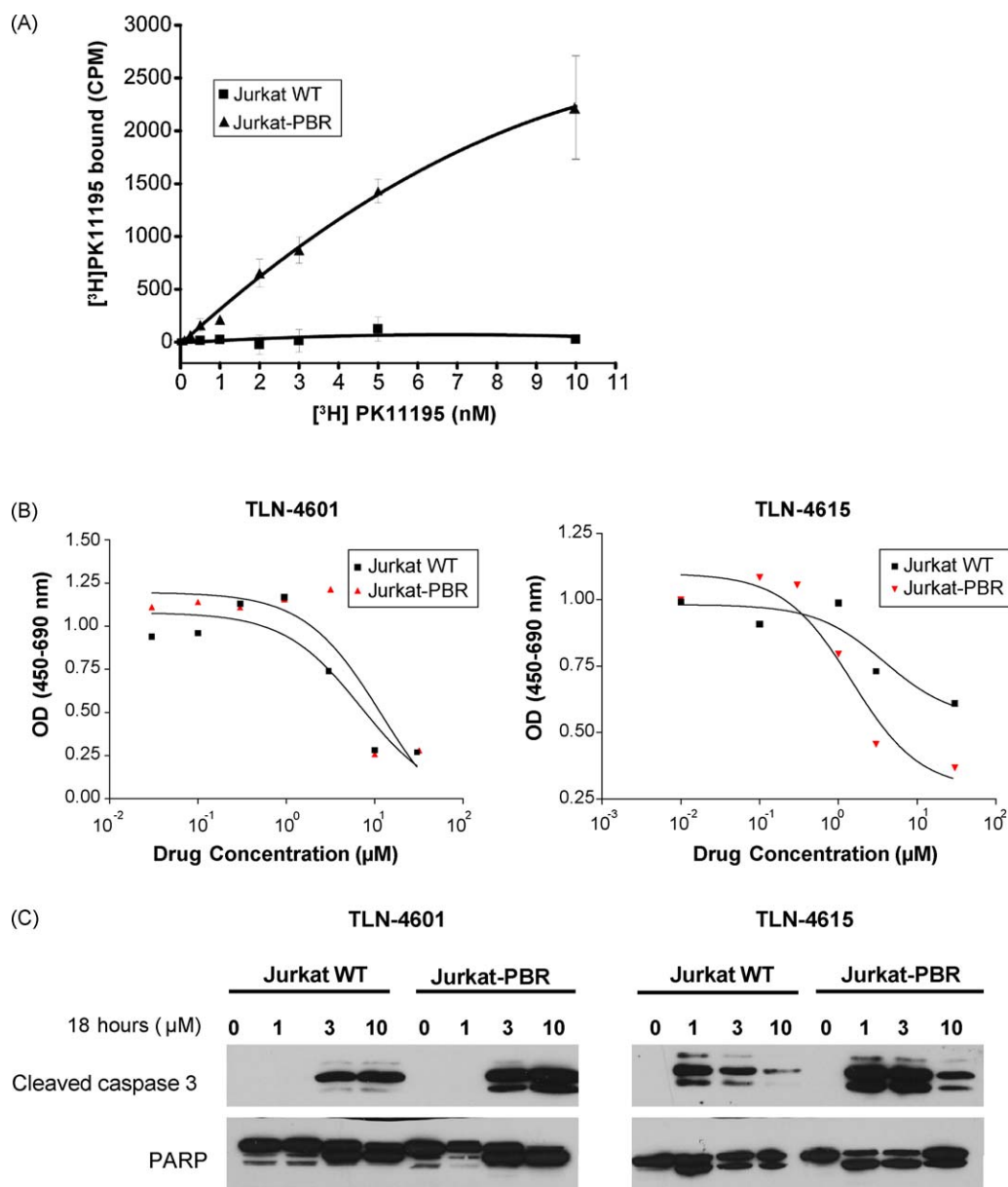


**Fig. 2.** PBR overexpression does not affect TLN-4601 and TLN-4615 cytotoxicity. (A) Saturation curves of specific [ $^3\text{H}$ ]PK11195 binding to Jurkat WT and Jurkat-PBR cells. Cell ( $40 \mu\text{g}$  of proteins) were incubated with increasing amounts of [ $^3\text{H}$ ]PK11195 with or without  $2 \mu\text{M}$  cold PK11195. Results are expressed as specific binding activity  $\pm$  S.D. (B) Viability of cells exposed for 3 days to various concentrations of TLN-4601 (left panel) or TLN-4615 (right panel) was assessed with an XTT assay. Reactions were done in triplicates three different times and representative results are shown. (C) Jurkat WT and Jurkat-PBR were exposed to 0, 1, 3 and  $10 \mu\text{M}$  TLN-4601 (left panel) or TLN-4615 (right panel) for 18 h and protein extracts assessed for caspase 3 and PARP cleavage by Western blots.

Jurkat WT and Jurkat-PBR cell lines, also resulted in caspase 3 activation and PARP cleavage (Fig. 2C, right panel). The induction of apoptosis is not due to incubation conditions since we did not observe caspase activation and PARP cleavage in cells treated with 0.05% DMSO for 18 h. These data strongly suggest that TLN-4601 and its closely related analog, TLN-4615, induce apoptosis independently of PBR binding.

TLN-4601 resulted in the translocation of Cytochrome C from the mitochondria to the cytosol, an early step in apoptosis induction, within 4 h in both cell lines following a 10  $\mu$ M time-course (Fig. 3A).  $\Psi$ M loss, a phenomenon witnessed alongside Cytochrome C release, was also similar in both cell lines (Fig. 3B). The decrease in cell viability as measured by trypan blue exclusion was similar in both cell lines. At the 24 h time point more than 95% of the cells were dead. The decrease in cell viability correlated with the appearance and increase in DNA nucleosomal fragmentation (Fig. 3C).

### 3.3. *In vivo* PBR occupancy by TLN-4601 in the rat C6 tumor orthotopic tumor model

Previous studies have shown that *in vivo* administration of [ $^3$ H]PK11195 to rats harbouring intracranial C6 gliomas, which are

documented to express high levels of PBRs, resulted in high levels of tritiated drug binding to the tumor with little binding to the adjacent normal brain tissue [32]. Moreover, this tumor specific binding was completely inhibited by preadministration of unlabeled PK11195 [32]. As our earlier studies indicated that TLN-4601 inhibited *in vitro* cell proliferation and *in vivo* tumor growth of rat C6 glioblastoma, we used this model system to determine if TLN-4601 could bind specifically to PBR *in vivo*.

The experimental design is detailed in Fig. 4A. Tumors were first imaged during 60 min following a bolus IV administration of [ $^{11}$ C]PK11195. TLN-4601 was then administered by an IV bolus infusion (30 mg/kg) followed by a continuous IV infusion (5 mg/kg/h) that lasted throughout the second scan and image acquisition. Using the simplified reference tissue method, we determined the mean tumor B.P. (baseline) =  $2.19 \pm 0.16$  (mean  $\pm$  SEM) and the mean B.P. (TLN-4601) =  $0.14 \pm 0.13$  (mean  $\pm$  SEM). After the continuous IV infusion, the PBR occupancy for [ $^{11}$ C](R)-PK11195 binding was reduced by an average of 91.67% ( $P < 0.0001$ ). The results presented in Fig. 4B and C, show that TLN-4601 attenuated [ $^{11}$ C]-PK11195 binding. These data indicate that TLN-4601 binds the PBR *in vivo* and confirm that TLN-4601 crosses the blood–brain barrier.

Steady-state plasma, liver, brain and brain tumor concentrations of TLN-4601 are shown in Fig. 4D. The data presented

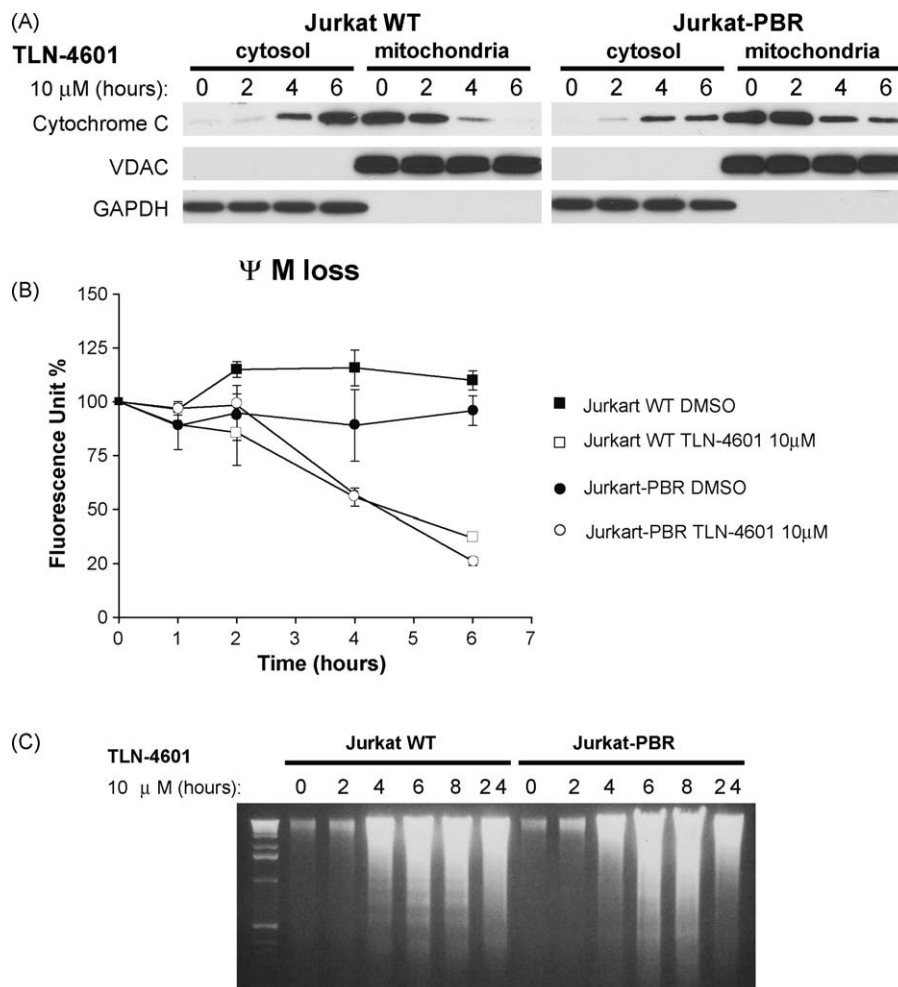


**Fig. 3.** Jurkat exposed to TLN-4601 commit to apoptosis independently from PBR expression. Jurkat WT and Jurkat-PBR exposed for various increasing times to 10  $\mu$ M TLN-4601 were analyzed for the three following apoptotic changes. Blots are representatives of three separate experiments. (A) Cytochrome C release was assessed after selective permeabilization with digitonin to obtain cytosolic and mitochondrial extracts. Western blots show the timing of Cytochrome C release and VDAC and GAPDH were used as loading controls for mitochondrial and cytosolic extracts, respectively. Blots are representatives of three separate experiments. (B)  $\Psi$ M loss was measured following TMRE staining and FACS analysis. Values shown represent the median fluorescence normalized for untreated cells at time 0. Assays were done in triplicates and error bars represent standard deviation (S.D.). (C) DNA fragmentation is shown following genomic DNA extraction and resolving on a 1.5% agarose TBE 1 $\times$  gel.

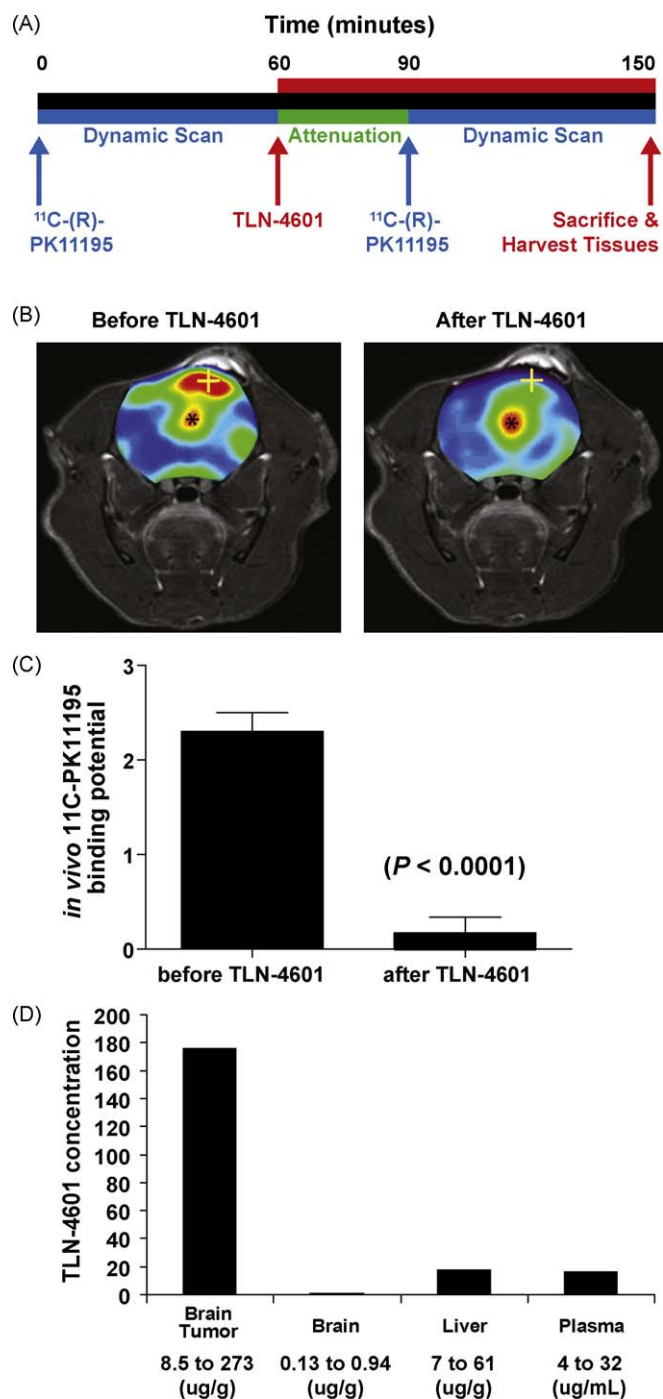


**Fig. 4.** *In vivo* PBR occupancy by TLN-4601 in the rat C6 tumor orthotopic model. (A) Schematic representation of the experimental design. Dynamic PET scan imaging of brains from rats surgically implanted with C6 glioma spheroids upon their brain were performed for 60 min following [ $^{11}\text{C}$ ](R)-PK11195 injection. TLN-4601 was then administered by a bolus IV infusion (30 mg/kg) followed by a continuous IV infusion (5 mg/h/kg) lasting for the duration of the second dynamic scan. (B) Representative images obtained from the PET scan before and after TLN-4601 treatment. The cross represents the tumor (C6-glioma), the asterisk likely represents a necrotic area and therefore non-specific binding of [ $^{11}\text{C}$ ](R)-PK11195. The blue region represents non-specific soft tissue of [ $^{11}\text{C}$ ](R)-PK11195. (C) Bar graph representation of the PET scan analysis (mean of 6 animals). (D) Bar graph representation of the tissue and plasma TLN-4601 concentrations. Following the completion of the *in vivo* studies, animals were sacrificed by anesthetic overdose and decapitated. Brain, tumor (excised from normal brain), and liver were snap-frozen in liquid nitrogen and stored at  $-80^\circ\text{C}$ . Blood samples were collected into  $\text{K}_2\text{-EDTA}$  tubes and stored frozen at  $-80^\circ\text{C}$ . TLN-4601 was extracted with acetone and quantified by HPLC-MS/MS. Values represent the range and mean of 6 different rats.

indicates that TLN-4601 preferentially accumulates in the tumor. Indeed, drug levels were  $>200$ -fold higher in the tumor compared to the normal brain. TLN-4601 accumulation in the tumor ( $176\ \mu\text{g}/\text{mL}$ ) was also significant compared to liver ( $24.8\ \mu\text{g}/\text{mL}$ ; 7-fold) and plasma ( $16.2\ \mu\text{g}/\text{mL}$ ; 11-fold).

#### 4. Discussion

TLN-4601 was discovered from a *Micromonospora* sp. by the use of Thallion's proprietary DECIPHER<sup>®</sup> discovery platform [17,33]. The dibenzodiazepinone core of the molecule is exceedingly rare among natural products. We have previously identified and characterized the antitumor properties of TLN-4601 [18]. In light of the dibenzodiazepinone, we had evaluated the binding properties of TLN-4601 on the benzodiazepine receptors and reported that TLN-4601 was a specific PBR ligand. This finding was further confirmed in this paper and interestingly the binding affinity for the PBR is not mediated by the dibenzodiazepinone core, but rather by the farnesyl side chain. This conclusion is demonstrated by the fact that TLN-4615, a semi-synthetic derivative of TLN-4601 where the farnesyl side chain is now saturated, does not bind the PBR.

In the present study, we show that Jurkat cells, which lack WT PBR expression, are as sensitive toward TLN-4601 as their PBR transfected counterpart, Jurkat-PBR. These findings suggest that the growth inhibitory activity of TLN-4601, measured by the XTT assay, is not mediated by the PBR binding properties. Although we do not know the exact cellular target for TLN-4601, our recent mechanistic studies indicate that TLN-4601 inhibits Ras-MAPK signaling pathway [34]. We show here that the effect of TLN-4601 on cell toxicity is mediated by the induction of apoptosis. Both in Jurkat WT and Jurkat-PBR, caspase 3 and PARP cleavage was observed after an overnight exposure to  $3\ \mu\text{M}$  of TLN-4601. There is a clear correlation between caspase 3 and PARP cleavage and cytotoxicity. DNA nucleosomal fragmentation, a hallmark of apoptosis, observed in both Jurkat WT and Jurkat-PBR, further confirms that TLN-4601 exposure induces apoptosis in both cell lines.

In a recent study, PBR expression was demonstrated in Jurkat cells [35]. The receptor had two amino acid substitutions and the resulting PBR protein, named JuPBR and said to be functional, had low-affinity binding sites for PK11195. While PK11195 has a high-affinity for WTPBR our data indicate that this is not the case for TLN-4601, which is shown here to have a low-affinity for the WTPBR. The concentrations of TLN-4601 used are close to the  $K_i$  value for the WT receptor and would be much too low to bind to JuPBR, which has 200-fold lower affinity towards PBR ligands [35]. Furthermore, the non-PBR binder TLN-4615 also induced apoptosis in Jurkat cells, indicated by the cleavage of caspase 3 and PARP (Fig. 2C). Taken together, these results indicate that TLN-4601 induces apoptosis in Jurkat cells, regardless of PBR expression levels.

The relationship between PBR ligand toxicity and their binding to PBR has been questioned due to the fact that they bind with nanomolar affinity but induce apoptosis in the high  $\mu\text{M}$  range [21,36,37]. Moreover, two independent studies using different PBR ligands and cell lines with low or high levels of PBR as well as the Jurkat WT and Jurkat-PBR demonstrated that PBR ligand-induced cell death is unrelated to their PBR-binding properties [25,38]. Although these ligands induce apoptosis, their actual cellular target is still undefined.

Several lines of evidence have alluded to the mPT as a critical event in mediating apoptosis [39]. mPT is a phenomenon by which the inner mitochondrial membrane (IMM) becomes permeable to molecules smaller than 1500 Da following mPT pore opening. In certain forms of intrinsic apoptosis, it has been proposed that the subsequent loss of ionic homeostasis caused matrix swelling and physical OMM rupture [40]. mPT pore opening would then lead to

the release of Cytochrome C into the cytosol from the intermembrane space of mitochondria, considered to be the “point of no return” and one of the early step in the intrinsic form of apoptosis. PBR has been suggested to be a constituent of this pore in association with VDAC and ANT, and to take part in the induction of apoptosis. In the present study, we show that TLN-4601 exposure decreased mitochondrial membrane potential ( $\Psi$ M). As the decrease was similar in Jurkat WT and Jurkat-PBR, it is unlikely to be linked to PBR binding. Cytochrome C release was observed in both cell lines between 2 and 4 h, which corresponds to the decrease in  $\Psi$ M. The mechanism by which TLN-4601 induces Cytochrome C release and a decrease in  $\Psi$ M is unknown at present.

The potential of PBR-targeted therapies in cancer has been proposed by the use of PBR ligand-drug conjugates [41,42]. Taking advantage of the fact that PBRs are selectively increased in both experimental and human brain tissues compared to normal brain and peripheral tissues [32,43] we examined whether TLN-4601 would preferentially target and accumulate in tumors using an intra-cerebral orthotopic tumor model in rats. As a model system we used the rat C6 glioma cells since they are known to express high levels of PBR and specific PBR ligands have been shown to inhibit their proliferation and induce apoptosis [36]. Moreover, we have shown that TLN-4601 inhibits the growth of rat C6 tumors both *in vitro* and *in vivo* [18]. The data obtained in the present study indicate that TLN-4601 can bind to the PBR *in vivo* as it minimized the binding of the selective and high-affinity ligand, [ $^{14}$ C]PK11195. Furthermore, we observed a 200-fold increase in TLN-4601 drug levels in brain tumor compared with the normal brain. Given that we utilized an orthotopic brain tumor model, and that TLN-4601 was administered by the tail vein, the data confirm our earlier findings suggesting that TLN-4601 crosses the blood–brain barrier. It is true that the implantation of tumor cells in the brain of normal rats somewhat impairs the blood–brain barrier and that the 200-fold higher levels could be partially due to leakiness of the model. On the other hand, the fact TLN-4601 brain tumor drug concentrations were 11-fold higher than those found in the plasma and liver is highly suggestive of preferential tumor uptake. Similar findings were observed with a gemcitabine-PK11195 conjugate, where a 2-fold enhancement in brain tumor selectivity was observed compared to gemcitabine alone [41]. Taken together with our earlier findings showing antitumor activity in rat and human glioma tumor xenograft models [18], these results support the use of TLN-4601 as a treatment for brain cancer.

In summary, the findings presented in this paper indicate that TLN-4601, a novel antitumor agent and PBR-ligand, induces apoptosis independently of PBR expression. As the compound accumulates in tumors having high levels of PBR, we propose that the PBR-binding property of TLN-4601 may potentiate its accumulation in cells overexpressing PBR, a promising property for an anticancer drug candidate.

## Acknowledgments

The authors would like to thank Eric Thibaudeau for FACS analysis, Zhizi Zhao for illustrations and Allan Mandelzys for critical review of the manuscript. Thierry Bertomeu and Val Zvereff were funded by NSERC IRD post-doctoral fellowships.

## References

- [1] Papadopoulos V, Baraldi M, Guilarte TR, Knudsen TB, Lacapere JJ, Lindemann P, et al. Translocator protein (18 kDa): new nomenclature for the peripheral-type benzodiazepine receptor based on its structure and molecular function. *Trends Pharmacol Sci* 2006;27:402–9.
- [2] Braestrup C, Squires RF. Specific benzodiazepine receptors in rat brain characterized by high-affinity (3H)diazepam binding. *Proc Natl Acad Sci USA* 1977;74:3805–9.
- [3] Gavish M, Bachman I, Shoukrun R, Katz Y, Veenman L, Weisinger G, et al. Enigma of the peripheral benzodiazepine receptor. *Pharmacol Rev* 1999;51:629–50.
- [4] Bernardi P, Krauskopf A, Basso E, Petronilli V, Blachly-Dyson E, Di Lisa F, et al. The mitochondrial permeability transition from *in vitro* artifact to disease target. *FEBS J* 2006;273:2077–99.
- [5] Papadopoulos V, Amri H, Boujrad N, Cascio C, Culty M, Garnier M, et al. Peripheral benzodiazepine receptor in cholesterol transport and steroidogenesis. *Steroids* 1997;62:21–8.
- [6] Galiegue S, Casellas P, Kramar A, Tinel N, Simony-Lafontaine J. Immunohistochemical assessment of the peripheral benzodiazepine receptor in breast cancer and its relationship with survival. *Clin Cancer Res* 2004;10:2058–64.
- [7] Maaser K, Grabowski P, Sutter AP, Hopfner M, Foss HD, Stein H, et al. Overexpression of the peripheral benzodiazepine receptor is a relevant prognostic factor in stage III colorectal cancer. *Clin Cancer Res* 2002;8:3205–9.
- [8] Han Z, Slack RS, Li W, Papadopoulos V. Expression of peripheral benzodiazepine receptor (PBR) in human tumors: relationship to breast, colorectal, and prostate tumor progression. *J Recept Signal Transduct Res* 2003;23:225–38.
- [9] Katz Y, Ben-Baruch G, Kloog Y, Menczer J, Gavish M. Increased density of peripheral benzodiazepine-binding sites in ovarian carcinomas as compared with benign ovarian tumours and normal ovaries. *Clin Sci (Lond)* 1990;78:155–8.
- [10] Hardwick M, Fertikh D, Culty M, Li H, Vidic B, Papadopoulos V. Peripheral-type benzodiazepine receptor (PBR) in human breast cancer: correlation of breast cancer cell aggressive phenotype with PBR expression, nuclear localization, and PBR-mediated cell proliferation and nuclear transport of cholesterol. *Cancer Res* 1999;59:831–42.
- [11] Beinlich A, Strohmeier R, Kaufmann M, Kuhl H. Relation of cell proliferation to expression of peripheral benzodiazepine receptors in human breast cancer cell lines. *Biochem Pharmacol* 2000;60:397–402.
- [12] Hardwick M, Cavalli LR, Barlow KD, Haddad BR, Papadopoulos V. Peripheral-type benzodiazepine receptor (PBR) gene amplification in MDA-MB-231 aggressive breast cancer cells. *Cancer Genet Cytogenet* 2002;139:48–51.
- [13] Miyazawa N, Hamel E, Diksic M. Assessment of the peripheral benzodiazepine receptors in human gliomas by two methods. *J Neurooncol* 1998;38:19–26.
- [14] Black KL, Ikezaki K, Toga AW. Imaging of brain tumors using peripheral benzodiazepine receptor ligands. *J Neurosurg* 1989;71:113–8.
- [15] Galiegue S, Tinel N, Casellas P. The peripheral benzodiazepine receptor: a promising therapeutic drug target. *Curr Med Chem* 2003;10:1563–72.
- [16] Zazopoulos E, Huang K, Staffa A, Liu W, Bachmann BO, Nonaka K, et al. A genomics-guided approach for discovering and expressing cryptic metabolic pathways. *Nat Biotechnol* 2003;21:187–90.
- [17] McAlpine JB, Banskota AH, Charan RD, Schlingmann G, Zazopoulos E, Pirae M, et al. Biosynthesis of diazepamomycin/ECO-4601, a Micromonospora secondary metabolite with a novel ring system. *J Nat Prod* 2008;71:1585–90.
- [18] Gourdeau H, McAlpine JB, Ranger M, Simard B, Berger F, Beaudry F, et al. Identification, characterization and potent antitumor activity of ECO-4601, a novel peripheral benzodiazepine receptor ligand. *Cancer Chemother Pharmacol* 2008;61:911–21.
- [19] Zisterer DM, Campiani G, Nacci V, Williams DC. Pyrrolo-1,5-benzoxazepines induce apoptosis in HL-60, Jurkat, and Hut-78 cells: a new class of apoptotic agents. *J Pharmacol Exp Ther* 2000;293:48–59.
- [20] Kessel D, Horwitz JP. Pro-apoptotic interactions between XK469 and the peripheral benzodiazepine receptor. *Cancer Lett* 2001;168:141–4.
- [21] Maaser K, Hopfner M, Jansen A, Weisinger G, Gavish M, Kozikowski AP, et al. Specific ligands of the peripheral benzodiazepine receptor induce apoptosis and cell cycle arrest in human colorectal cancer cells. *Br J Cancer* 2001;85:1771–80.
- [22] Decaudin D, Castedo M, Nematí F, Beurdeley-Thomas A, De Pinieux G, Caron A, et al. Peripheral benzodiazepine receptor ligands reverse apoptosis resistance of cancer cells *in vitro* and *in vivo*. *Cancer Res* 2002;62:1388–93.
- [23] Sutter AP, Maaser K, Hopfner M, Barthel B, Grabowski P, Faiss S, et al. Specific ligands of the peripheral benzodiazepine receptor induce apoptosis and cell cycle arrest in human esophageal cancer cells. *Int J Cancer* 2002;102:318–27.
- [24] Li J, Wang J, Zeng Y. Peripheral benzodiazepine receptor ligand, PK11195 induces mitochondria cytochrome c release and dissipation of mitochondria potential via induction of mitochondria permeability transition. *Eur J Pharmacol* 2007;560:117–22.
- [25] Hans G, Wislet-Gendebien S, Lallemand F, Robe P, Rogister B, Belachew S, et al. Peripheral benzodiazepine receptor (PBR) ligand cytotoxicity unrelated to PBR expression. *Biochem Pharmacol* 2005;69:819–30.
- [26] Carayon P, Portier M, Dussosoy D, Bord A, Petitpretre G, Canat X, et al. Involvement of peripheral benzodiazepine receptors in the protection of hematopoietic cells against oxygen radical damage. *Blood* 1996;87:3170–8.
- [27] Janssen MJ, Ensing K, de Zeeuw RA. Improved benzodiazepine radioreceptor assay using the MultiScreen Assay System. *J Pharm Biomed Anal* 1999;20:753–61.
- [28] Waterhouse NJ, Trapani JA. A new quantitative assay for cytochrome c release in apoptotic cells. *Cell Death Differ* 2003;10:853–5.
- [29] Walker PR, Kwast-Welfeld J, Gourdeau H, Leblanc J, Neugebauer W, Sikorska M. Relationship between apoptosis and the cell cycle in lymphocytes: roles of protein kinase C, tyrosine phosphorylation, and AP1. *Exp Cell Res* 1993;207:142–51.
- [30] Del Duca D, Werbowetski T, Del Maestro RF. Spheroid preparation from hanging drops: characterization of a model of brain tumor invasion. *J Neurooncol* 2004;67:295–303.

- [31] Kropholler MA, Boellaard R, Schuitemaker A, Folkersma H, van Berckel BN, Lammertsma AA. Evaluation of reference tissue models for the analysis of [<sup>11</sup>C](R)-PK11195 studies. *J Cereb Blood Flow Metab* 2006;26:1431–41.
- [32] Starosta-Rubinstein S, Ciliax BJ, Penney JB, McKeever P, Young AB. Imaging of a glioma using peripheral benzodiazepine receptor ligands. *Proc Natl Acad Sci USA* 1987;84:891–5.
- [33] Bachmann BO, McAlpine JB, Zazopoulos E, Farnet CM, Pirae M. Farnesyl dibenzodiazepinones, processes for their production and their use as pharmaceuticals. US Patent No. 7,101,872; 2004.
- [34] Bouffaied N, Wioland M-A, Falardeau P, Gourdeau H. TLN-4601, a novel anticancer agent, inhibits Ras signalling post Ras prenylation and prior to MEK activation. *Anti-Cancer Drugs* 2010;21:543–52.
- [35] Costa B, Salvetti A, Rossi L, Spinetti F, Lena A, Chelli B, et al. Peripheral benzodiazepine receptor: characterization in human T-lymphoma Jurkat cells. *Mol Pharmacol* 2006;69:37–44.
- [36] Chelli B, Lena A, Vanacore R, Da Pozzo E, Costa B, Rossi L, et al. Peripheral benzodiazepine receptor ligands: mitochondrial transmembrane potential depolarization and apoptosis induction in rat C6 glioma cells. *Biochem Pharmacol* 2004;68:125–34.
- [37] Maaser K, Sutter AP, Scherubl H. Mechanisms of mitochondrial apoptosis induced by peripheral benzodiazepine receptor ligands in human colorectal cancer cells. *Biochem Biophys Res Commun* 2005;332:646–52.
- [38] Gonzalez-Polo RA, Carvalho G, Braun T, Decaudin D, Fabre C, Larochette N, et al. PK11195 potentially sensitizes to apoptosis induction independently from the peripheral benzodiazepine receptor. *Oncogene* 2005;24:7503–13.
- [39] Brenner C, Grimm S. The permeability transition pore complex in cancer cell death. *Oncogene* 2006;25:4744–56.
- [40] Javadov S, Karmazyn M. Mitochondrial permeability transition pore opening as an endpoint to initiate cell death and as a putative target for cardioprotection. *Cell Physiol Biochem* 2007;20:1–22.
- [41] Guo P, Ma J, Li S, Guo Z, Adams AL, Gallo JM. Targeted delivery of a peripheral benzodiazepine receptor ligand-gemcitabine conjugate to brain tumors in a xenograft model. *Cancer Chemother Pharmacol* 2001;48:169–76.
- [42] Trapani G, Laquintana V, Latrofa A, Ma J, Reed K, Serra M, et al. Peripheral benzodiazepine receptor ligand-melphalan conjugates for potential selective drug delivery to brain tumors. *Bioconjug Chem* 2003;14:830–9.
- [43] Black KL, Ikezaki K, Santori E, Becker DP, Vinters HV. Specific high-affinity binding of peripheral benzodiazepine receptor ligands to brain tumors in rat and man. *Cancer* 1990;65:93–7.